SIMULATION OF AUTOMOTIVE AC-DC MACROCOMMUTATOR GENERATORS

Józef Tutaj

Krakow University of Technology
Department of Mechanical Engineering, Mechatronics Institution
Warszawska Street 24, 31-155 Krakow, Poland
phone: +48 12 6283323, fax: +48 12 6282071
e-mail: pmtutaj@cyf-kr.edu.pl

Abstract

This paper deals with PSPICE simulation of automotive AC-DC macrocommutator generators, in which are commonly equipped internal combustion engines and/or external combustion engines of civil and military automotive vehicles. In the beginning a physical model of automotive AC-DC macrocomutator generators is created. Next, on the basis of this physical model, a mathematical model of automotive AC-DC macrocommutator generators has been formulated, taking into account controlled nonlinear self-inductances and mutual-inductances. The created physical model for simulation of an automotive AC-DC macrocommutator generator with a diode macrocommutator (macroelectronic commutator) can be used, not only for the estimation of power quality (PQ) indices in these on-board 42 V_{DC} AC-DC commutator generators, but also for the investigation of new configurations of macrocommutators with fully-controllable uni- and/or bipolar electrical valves (e.g., with MOSFETs, IGBTs or MCTs). To estimate the AC output of the macrocommutator, as regards a power quality (PQ), the Fourier analysis of a phase current has been used. It can be concluded from the simulation results that a significantly lower harmonic content, especially, in the low-frequency range can be obtained using fully-controllable macrocommutators. Simulation results are presented, not only for an automotive electrical machine, but also for an AC-DC macrocommutator. The PSPICE simulation makes it possible to observe the static and transient oscillograms of different physical values (e.g., voltages and currents) which are not measurable in real electrical machines.

Keywords: *DC electrical machine, electronic commutator , integrated generator/starter, automotive generator*

1. Mathematical model

A mathematical model of a salient-pole, electrical machine can be presented in the following form [8, 10]:

$$
\begin{aligned}
&-2\omega\begin{bmatrix} L_m\sin 2\theta & L_n\sin(2\theta-\frac{2\pi}{3}) & L_n\sin(2\theta-\frac{4\pi}{3}) & \frac{1}{2}L_\mu\sin\theta \\ L_n\sin(2\theta-\frac{2\pi}{3}) & L_m\sin(2\theta-\frac{4\pi}{3}) & L_n\sin 2\theta & \frac{1}{2}L_\mu\sin(\theta-\frac{2\pi}{3}) \\ L_n\sin(2\theta-\frac{4\pi}{3}) & L_n\sin 2\theta & L_m\sin(2\theta-\frac{2\pi}{3}) & \frac{1}{2}L_\mu\sin(\theta-\frac{4\pi}{3}) \\ \frac{1}{2}L_\mu\sin\theta & \frac{1}{2}L_\mu\sin(\theta-\frac{2\pi}{3}) & \frac{1}{2}L_\mu\sin(\theta-\frac{4\pi}{3}) & 0 \end{bmatrix}\begin{bmatrix} i_1 \\ i_2 \\ i_3 \\ i_4 \end{bmatrix}+ \\
&+\begin{bmatrix} L_\sigma+L_m\cos 2\theta & -L_\varsigma+L_n\cos(2\theta-\frac{2\pi}{3}) & -L_\varsigma+L_n\cos(2\theta-\frac{4\pi}{3}) & L_\mu\cos\theta \\ -L_\varsigma+L_n\cos(2\theta-\frac{2\pi}{3}) & L_\sigma+L_m\cos(2\theta-\frac{4\pi}{3}) & -L_\varsigma+L_n\cos 2\theta & L_\mu\cos(\theta-\frac{2\pi}{3}) \\ -L_\varsigma+L_n\cos(2\theta-\frac{4\pi}{3}) & -L_\varsigma+L_n\sin 2\theta & L_\sigma+L_m\cos(2\theta-\frac{2\pi}{3}) & L_\mu\cos(\theta-\frac{4\pi}{3}) \\ L_\mu\cos\theta & L_\mu\cos(\theta-\frac{2\pi}{3}) & L_\mu\cos(\theta-\frac{4\pi}{3}) & L_4 \end{bmatrix}\frac{d}{dt}\begin{bmatrix} i_1 \\ i_2 \\ i_3 \\ i_4 \end{bmatrix}+ \\
&+\begin{bmatrix} R_1 & 0 & 0 & 0 \\ 0 & R_2 & 0 & 0 \\ 0 & 0 & R_3 & 0 \\ 0 & 0 & 0 & R_4 \end{bmatrix}\begin{bmatrix} i_1 \\ i_2 \\ i_3 \\ i_4 \end{bmatrix}+\begin{bmatrix} 0 & 0 & 0 & 0 \\ 0 & 0 & 0 & 0 \\ 0 & 0 & 0 & 0 \\ 0 & 0 & 0 & \Delta U_4 \end{bmatrix} sign\begin{bmatrix} i_1 \\ i_2 \\ i_3 \\ i_4 \end{bmatrix}=\begin{bmatrix} U_1 \\ U_2 \\ U_3 \\ U_4 \end{bmatrix}. \qquad (1)
\end{aligned}
$$

The structure of matrices in Equation (1) creates a basic problem in further analytical investigation of dynamical properties of the electrical system under consideration [3-5]. The matrix elements are explicit functions of a generalised mechanical coordinate, hence, a function of time.

In this paper, the author solves the Equation (1) by means of a computer simulation in the real coordinates frame. To solve the differential Equation (1), physical models of a controlled nonlinear self-inductance and of a controlled nonlinear mutual inductance must be created first.

2. Physical models of a controlled nonlinear self-inductance and controlled mutual inductance

An electrical diagram of the controlled nonlinear self-inductance physical model is presented in Fig. 1a as an electrical subcircuit. The input terminals 1, 2 are connected across to an independent voltage source which changes accordingly to a desired change in the inductance, $L_{kk}(\theta)$, and the output terminals 3, 4 are connected across to the control voltage, referencing an instantaneous value $\omega\partial L_{kk}(\theta)/\partial\theta$ (an influence of feedbacks is shown in figure with the arrows). The terminals 7 and 8 are outputs of the controlled self-inductance where as a reference inductance is connected to the terminals 5, 6.

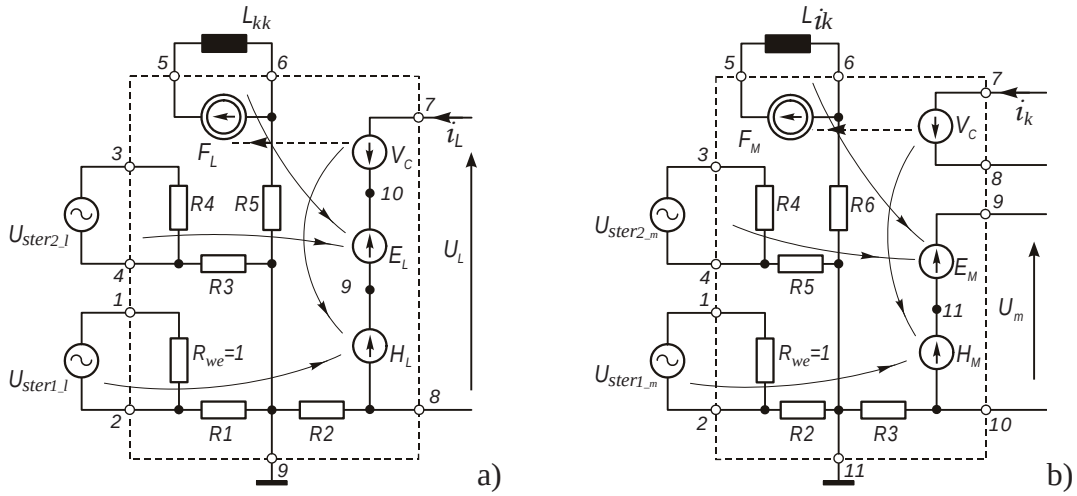

Fig. 1. Electrical diagrams of physical models: a) controlled self-inductance, b) controlled mutual inductance

This physical model of a controlled self-inductance can be extended for some applications by an addition of independent controlling voltage sources to take into account other factors that may affect the value of the self-inductance (e.g., current, temperature, geometrical asymmetry, etc.).

The physical model of the mutual inductance has the input terminals 1, 2 which are connected across to a voltage source that controls the magnetic coupling coefficient, $L_{ik}(\theta)$, and the output terminals 3, 4 are connected across to the control voltage, referencing an instantaneous value $\omega\partial L_{ik}(\theta)/\partial\theta$. The reference mutual inductance terminals 5, 6 are connected across to a current source F_M, which is controlled by the current terminals 7, 8 of the branch that contains the other magnetically - coupled inductance (see Fig. 1b).

3. Simulation physical model of an AC salient-pole electromagnetically excited generator

A physical model of the AC salient-pole electromagnetically excited generator [1, 2] is presented as an equivalent circuit in Fig. 2. It is derived from Equation (1) using the physical models of the self-inductance and the mutual inductance. A symmetrical resistive and inductive load has been assumed for the electrical machine. The initial simplifying assumptions about the electrical machine symmetry can be easily omitted to taking into account the asymmetry of electrical parameters (winding

resistances, self and mutual inductances or even geometrical changes in reference inductances and initial phase angles of voltages which to control self and mutual inductances).

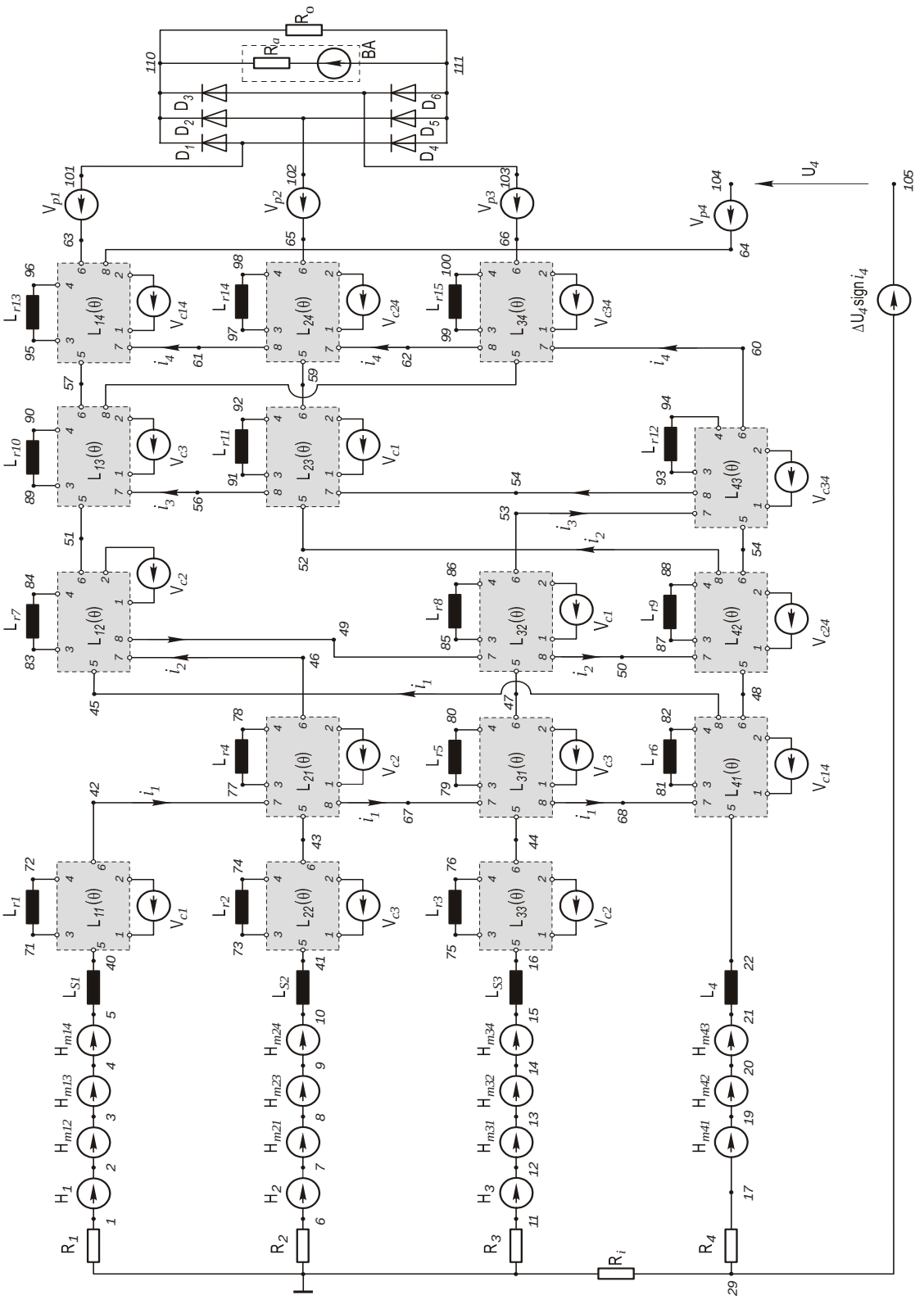

Fig. 2. Simulation physical model of an AC salient-pole, electromagnetically-excited generator with the diode AC-DC macroelectronic commutator

The digital simulation makes it possible to observe the type of changes and values of particular voltages, which are not measurable in a real electrical machine (Fig. 7a).

4. Time-domain waveforms of voltages and currents in an AC-DC macrocommutator generator with the diode macroelectronic commutator

Recently, on-board $42V_{DC}$, AC-DC macrocommutator generators with the diode macroelectronic commutator are the most commonly used in automotive vehicles. Fig. 3 shows selected waveforms of voltages and currents of a physical model of the AC-DC macrocommutator generator with a resistive load. This simulation physical model allows for obtaining, among others, time-domain waveforms of voltages and currents in self and mutual inductances of the armature or the field windings as well as particular waveforms of voltages and/or currents both in the field winding and in the macroelectronic commutator. Selected waveforms in characteristic points of the circuit are shown below. The Fig. 3 depicts time-domain waveforms of voltages across particular inductances of the field winding. The waveforms exhibit a high content of harmonics (especially in the voltage across the leakage inductance) which is caused by a steep rise of phase currents during the turn-on and/or turn-off of the uncontrolled electrical valves (diodes in the macroelectronic commutator). The sudden rise and fall of phase currents causes fast time-domain changes of the magnetic field in the field-winding magnetic circuit, which in turn increases iron losses. Time-domain waveforms of AC-DC macrocommutator generator's different voltages and currents are shown in Fig. 3-8.

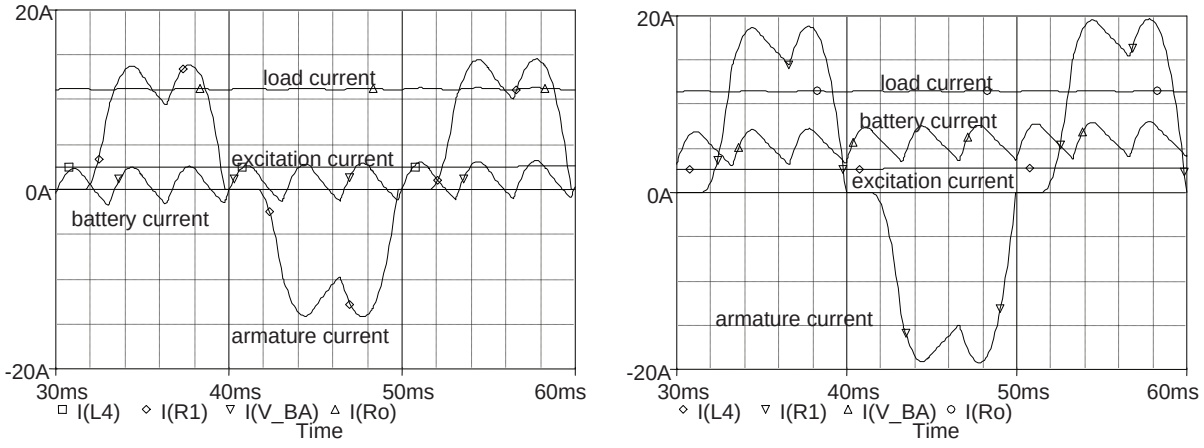

(a) (b)

Fig. 3. Time-domain waveforms of currents in the AC-DC macrocommutator generator's circuits at frequency of 50 Hz: for small values of the excitation current; (b) for great values of the excitation current

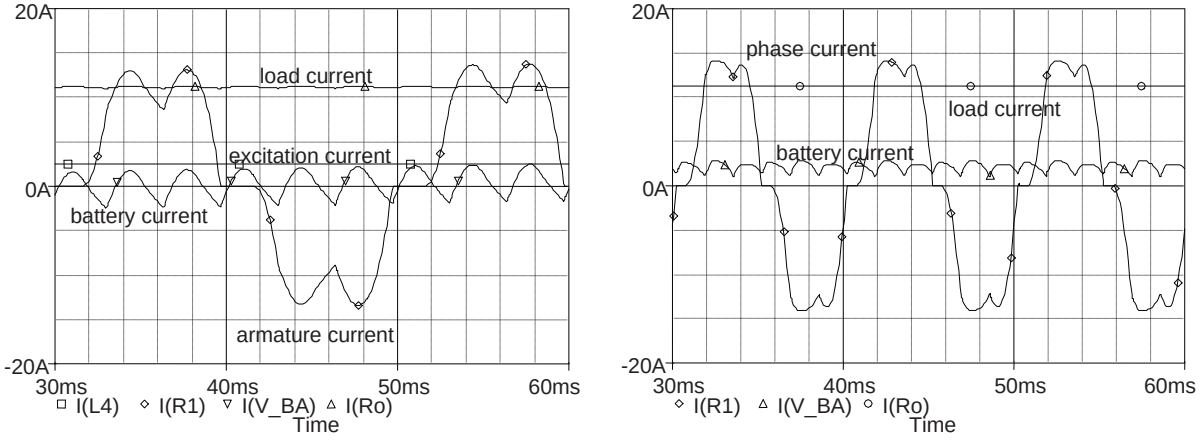

(a) (b)

Fig. 4. Time-domain waveforms of currents in the AC-DC macrocommutator generator's circuits: (a) for small values of the excitation current at frequency of 50 Hz; (b) for small values of the excitation current at frequency of 100 Hz

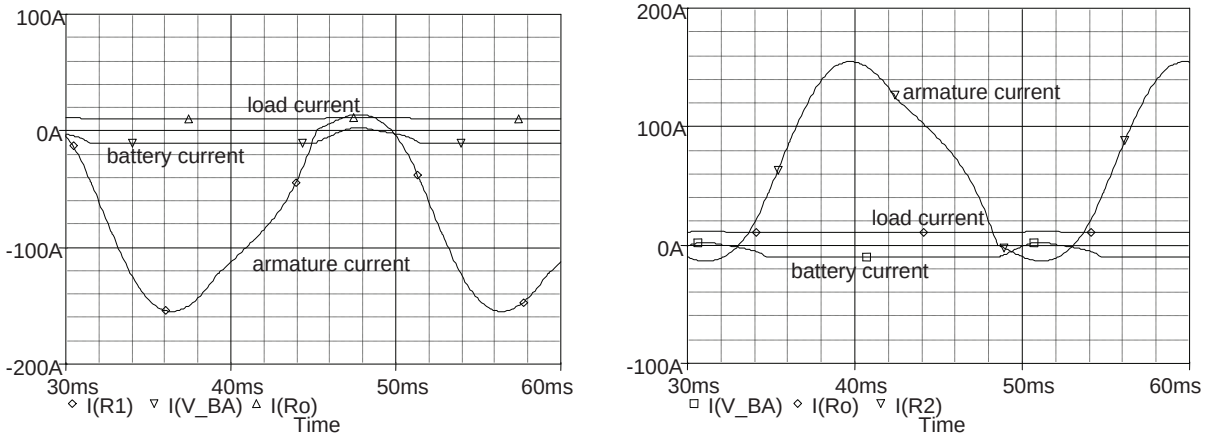

(a) (b)

Fig. 5. Time-domain waveforms of currents in the AC-DC macrocommutator generator's circuits at frequency 50 Hz: (a) for a short-circuit of a diode in the cathode commutating group; (b) for a short-circuit of a diode in the anode commutating group

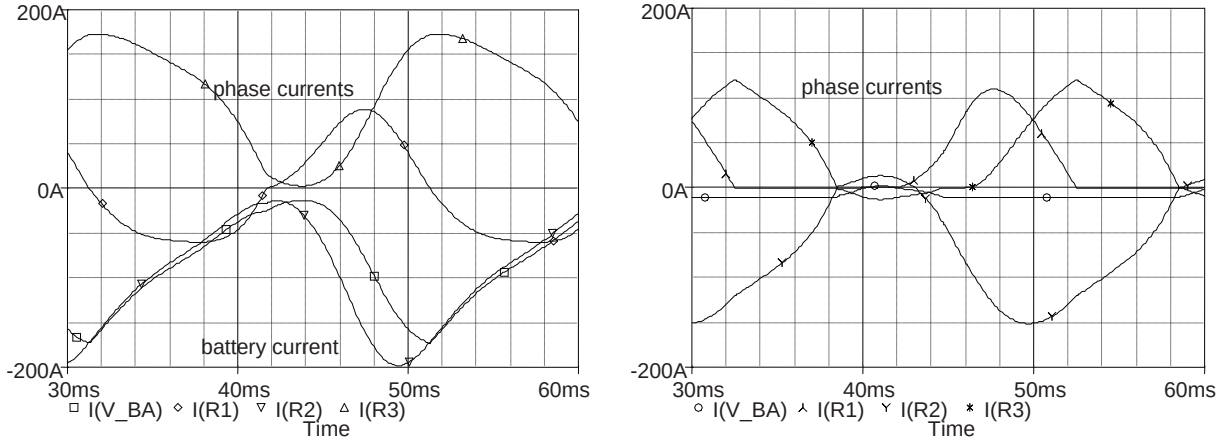

(a) (b)

Fig. 6. Time-domain waveforms of currents in the AC-DC macrocommutator generator's circuits at frequency 50 Hz: for a short-circuit of a one diode from the cathode commutating group; (b) for a short-circuit of an other diode from the anode commutating of group of the different phases

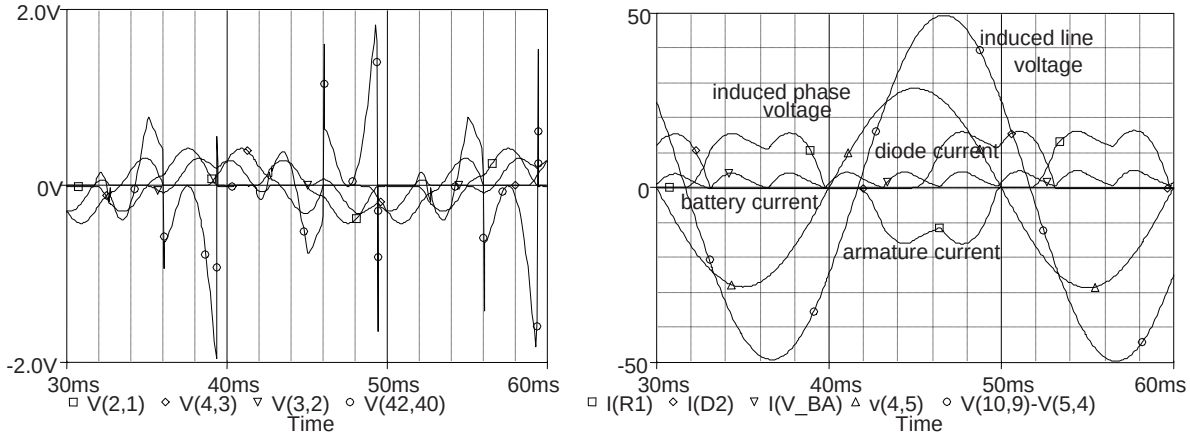

(a) (b)

Fig. 7. Time-domain waveforms of voltages and currents in selected components of the AC-DC macrocommutator generator

5. Power quality

To estimate the AC side power quality (PQ), the Fourier analysis of a phase current is shown in Tab. 1. The PSPICE simulation package allows for computation of the DC component and the first nine Fourier's harmonic components of a given voltage or current waveform. A set of columns presents the following parameters for each harmonic component: frequency, amplitude, ratio of the amplitude to the amplitude of the fundamental, phase shift, and phase shift with respect to the fundamental component. The last row of the table gives the total harmonic distortion (THD) expressed in percents.

Tab. 1. Fourier components of transient responses

FOURIER COMPONENTS OF TRANSIENT RESPONSE I(R1)
DC COMPONENT = 1.221838E-01

HARMONIC NO	FREQUENCY (HZ)	FOURIER COMPONENT	NORMALIZED COMPONENT	PHASE (DEG)	NORMALIZED PHASE (DEG)
1	5.000E+01	1.646E+01	1.000E+00	1.617E+02	0.000E+00
2	1.000E+02	9.699E-02	5.893E-03	-1.362E+02	-4.597E+02
3	1.500E+02	3.892E-02	2.365E-03	-1.624E+02	-6.476E+02
4	2.000E+02	4.088E-02	2.484E-03	1.677E+02	-4.791E+02
5	2.500E+02	3.798E+00	2.307E-01	-9.591E+01	-9.045E+02
6	3.000E+02	1.173E-02	7.125E-04	-1.472E+02	-1.118E+03
7	3.500E+02	6.156E-01	3.740E-02	-1.033E+02	-1.235E+03
8	4.000E+02	1.272E-02	7.731E-04	-1.015E+02	-1.395E+03
9	4.500E+02	7.427E-03	4.513E-04	-1.404E+02	-1.596E+03

TOTAL HARMONIC DISTORTION = 2.338463E+01 PERCENT

FOURIER COMPONENTS OF TRANSIENT RESPONSE V(101,102)
DC COMPONENT = -4.399159E-02

HARMONIC NO	FREQUENCY (HZ)	FOURIER COMPONENT	NORMALIZED COMPONENT	PHASE (DEG)	NORMALIZED PHASE (DEG)
1	5.000E+01	4.522E+01	1.000E+00	1.458E+02	0.000E+00
2	1.000E+02	1.055E-01	2.334E-03	-1.779E+02	-4.696E+02
3	1.500E+02	1.439E-01	3.181E-03	1.022E+02	-3.352E+02
4	2.000E+02	9.322E-02	2.062E-03	2.545E+01	-5.578E+02
5	2.500E+02	6.432E+00	1.423E-01	-1.627E+02	-8.918E+02
6	3.000E+02	1.581E-01	3.497E-03	-7.414E+01	-9.491E+02
7	3.500E+02	3.378E+00	7.472E-02	1.399E+02	-8.809E+02
8	4.000E+02	1.050E-01	2.323E-03	-1.660E+02	-1.333E+03
9	4.500E+02	1.396E-01	3.087E-03	1.206E+02	-1.192E+03

TOTAL HARMONIC DISTORTION = 1.608274E+01 PERCENT

An amplitude spectrum of a selected physical quantity in the electrical energy distribution system of the AC-DC macrocommutator generator can be also obtained. This is shown in Fig. 8.

Time-domain waveforms of a phase current and a line-to-line voltage at the macrocommutator's input have been selected for Fourier harmonic analysis. These physical quantities are easily measurable in an on-board AC-DC macrocommutator generator.

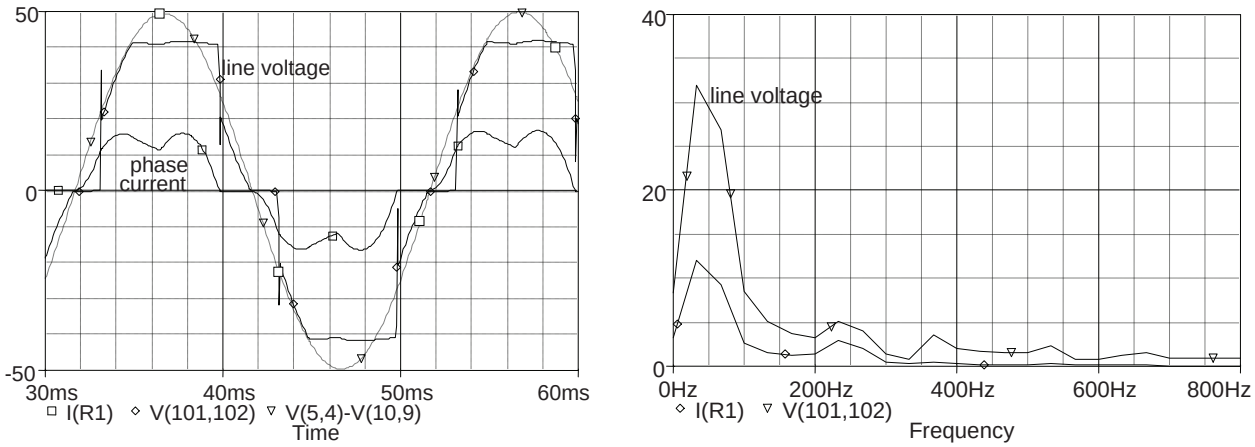

(a) (b)

Fig. 8. Time-domain waveforms of voltages and currents in the AC-DC macrocommutator generator (a) a phase voltage and a phase current; (b) amplitude spectrum of a line voltage and phase current

6. Conclusions

From computer-simulation results of harmonic analysis of a phase current in an armature winding of the AC-DC macrocommutator generator with a diode macroelectronic commutator (Fig. 8) above presented, it can be seen that there is a high content of odd harmonics.

From the above-mentioned results, it can be concluded that a significantly lower harmonic content (especially in the low-frequency range) can be obtained using fully controlled macro-commutators (e.g., with MOSFETs, IGBTs, IGCTs or MCTs), which are using fully controllable electrical valves. The simulation physical model created for the automotive AC-DC macrocommutator generator with a diode macroelectronic commutator can be used not only for estimation of PQ indices in these AC-DC macrocommutator generators but also for investigation of new configurations of macro-electronic commutators [7, 9].

References

[1] Adler, U. (Ed.), *Automotive Electric/Electronic Systems*, Bosch – VDI Verlag, Duesseldorf 1988.
[2] BOSCH, *Automotive Electric/Electronic Systems*, VDI Verlag, Düsseldorf 2005.
[3] Fijałkowski, B., *Mathematical models of select-ed aviation and automotive discrete dynamical systems*, Monografia 53, Politechnika Krakowska im. Tadeusza Kosciuszki, p. 276 Krakow 1987.
[4] Koziej, E., *Maszyny elektryczne pojazdów samochodowych*, WNT, Warszawa 1981.
[5] Skwarczyński, J., *Identyfikacja parametrów modelu maszyny synchronicznej dla stanów dynamicznych*, Kraków 1976.
[6] Tutaj, J., *Artificial Intelligence Voltage Control System for Automotive Generators*, 8th International Symposium on Artificial Intelligence Based Measurement and Control (AIMaC'91) Proceedings, Ritsumeikan University, Kyoto, Japan, September 12-16, 1991, pp. 475-480, Kyoto 1991.
[7] Tutaj, J., *A Novel Three-Phase Bridge AC-to-DC Converter Configuration*, International Conference on Electrical Drives and Power Electronics Proceedings (ED&PE), Vol. 1, pp. 252-255, Kosice 1992.
[8] Tutaj, J., *PSPICE the AC-DC Commutator On-board 42V Generator Simulation*, Proceedings of the Automotive & Transportation Technology Congress (ATT), No. 2002-01-2239, Paris 2002.
[9] Tutaj, J., *Transistor rectifiers for the automotive DC generators*, KONMOT-Autoprogres, Motoryzacja w dobie zrównoważonego rozwoju świata, pp. 245-253, Szczawnica 2008.

[10] Tutaj J., *A mathematical model of the generator/starter for automotive vehicle*, Journal of KONES Powertrain and Transport, Vol. 16 No.1 2009, pp. 495-506, Warsaw 2009.